

One-Step Nanocasting Synthesis of Highly Ordered Single Crystalline Indium Oxide Nanowire Arrays from Mesostructured Frameworks

Haifeng Yang, Qihui Shi, Bozhi Tian, Qingyi Lu, Feng Gao, Songhai Xie, Jie Fan, Chengzhong Yu, Bo Tu, and Dongyuan Zhao*

Laboratory of Molecular Catalysis and Innovative Materials, Department of Chemistry, Fudan University, Shanghai 200433, P. R. China

Received January 2, 2003; E-mail: dyzhao@fudan.edu.cn

Indium oxide, an important transparent conductive oxide (TCO) with a wide band gap close to GaN, has been well studied in past years because of its application in solar cells, solid-state optoelectronic devices, and so on.^{1,2} Research on nanoparticles and structures of In_2O_3 is still quite sparse;³ however, the possible applications of In_2O_3 nanostructures for ultraviolet–visible (UV) lasers, detectors, and gas sensors are extremely fascinating.⁴

Nanocasting by using three-dimensional (3D) mesostructured silica as hard templates is one of the most important strategies for synthesizing highly ordered non-siliceous mesoporous materials or nanowire arrays.⁵ As previously reported, inorganic precursors can be incorporated into the channels of mesoporous silica by sorption, phase transition, ion exchange, or complex or covalent grafting and form an inorganic framework by further treatments. However, after removal of the silica template, the ordered mesostructure is seldom maintained because the inorganic precursors are inclined to be absorbed on the external surface of templates and the channels are not completely filled, which causes the framework formed inside the pores to be lacking in sufficient internal cross-linkage. Until now, only ordered mesoporous carbon and metals were derived.^{5–10}

In this paper, we demonstrate a one-step nanocasting route to prepare highly ordered single-crystal indium oxide nanowire (IONW) arrays with mesostructured frameworks. Unlike the reported multistep nanocasting process (synthesis of mesoporous materials, and then incorporation of precursors and formation of inorganic frameworks), a highly ordered mesostructured surfactant-silica monolith with low external surface serves as both the template and the reducing agent and makes the formation of single-crystal IONWs in its channels easily in one step by using normal $\text{In}(\text{NO}_3)_3$ as an inorganic precursor. After silica is removed, highly ordered uniform single-crystal IONW arrays with hexagonal ($p6mm$) or cubic ($la3d$) mesostructures are derived. To the best of our knowledge, this is the first report of a single crystalline mesostructured In_2O_3 framework.

The typical preparation procedure is shown in Scheme 1 (Supporting Information, SI). First, by adding $\text{In}(\text{NO}_3)_3$ directly into the batch, In^{3+} doped silica/surfactant mesostructured monoliths were prepared through a liquid paraffin protected fast evaporation method developed by us previously¹¹ and by using a triblock copolymer as a template (see SI). After being calcined at 550 °C in air to remove the surfactants, highly ordered single-crystal IONWs were formed in the channels. The silica was dissolved by 2 M NaOH; energy-dispersive X-ray spectra (see SI) at all areas show the final product is a nearly pure In_2O_3 framework.

Highly ordered In^{3+} doped silica/surfactant mesostructured composites can be obtained by our one-step synthesis route when the mass ratio of In to Si is less than 1:2 in the initial reaction composition. After calcination, small angle XRD patterns show that the long-range order of the sample is completely retained (see SI). Because of the addition of metal salts, the pore size of the product

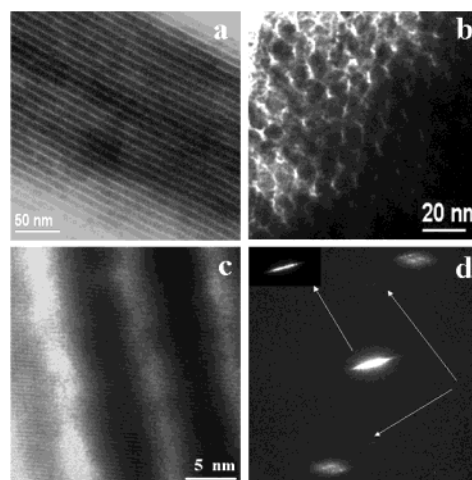


Figure 1. TEM images of In_2O_3 nanowire arrays with hexagonal mesostructure along the (a) [100] and (b) [001] directions; (c) HRTEM image along the [100] direction and (d) the corresponding SAED pattern.

increases a little (see SI). For the final silica-free sample, the high-angle XRD pattern shows well-resolved peaks for its high crystallinity, which can be indexed to a body-centered cubic (bcc) structure with a lattice constant of $a = 1.01$ nm.¹² The broad peak at about $2\theta \approx 22^\circ$ caused by amorphous silica is not detected after the removal of silica, also proving the purity of In_2O_3 .

By the one-step nanocasting route at 60 °C, highly ordered single-crystal IONW arrays with a hexagonal mesostructure were prepared. The In_2O_3 mesostructured framework was constructed by hexagonally packing nanowire arrays (Figure 1a,b).⁹ These nanowires are quite uniform in diameter (ca. 7.0 nm) due to the confined growth in the channels of the mesoporous silica template. The nanowires are confirmed to be single crystalline with the high-resolution TEM (HRTEM) images (Figure 1c), and the d spacing of the observed crystallographic plane is ca. 0.41 nm (211 reflection). These nanowires are interconnected by small irregular distributed rodlike metal oxides as can be revealed in HRTEM images (not shown here).¹⁰ Selected-area electron diffraction (SAED) (Figure 1d) shows obviously two sets of diffraction patterns caused by the long-range ordered mesostructure and the single-crystal nanowires, respectively. The diffused spots (single arrow and the inset) in the perpendicular direction of the channels are due to the 9.7 nm periodicity of the mesostructure (d_{100}), while the other spots (two arrows) are attributed to the 0.59 nm periodicity of the (111) crystallographic plane of the single-crystal IONWs. In addition, SEM results show that the samples possess a uniform rodlike morphology with a length of 1.0–2.5 μm and a diameter of 0.3–0.4 μm , and the yield is estimated to be higher than 98% (based on indium), which is well according to the highly ordered single-crystal IONW arrays with a hexagonal mesostructure.

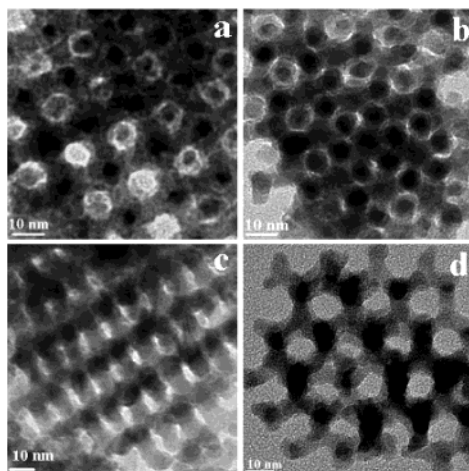


Figure 2. TEM images of the cubic $Ia3d$ mesostructured In_2O_3 framework along the (a) [100], (b) [111], and (c) [311] directions. (d) TEM images of the cubic (possible $I432$) mesostructured In_2O_3 framework along the [111] direction.

The formation mechanism of the In_2O_3 mesostructure can be postulated on the basis of these experimental results. Calcined with the surfactant, $\text{In}(\text{NO}_3)_3$ pyrolyzes to indium nanoparticles first. Because of the low melting point of the metal (160 °C), indium nanoparticles can shift easily inside the 1D channels of the silica monolith template that has almost no external surface areas; therefore, the indium nanoparticles can be aggregated in a certain segment to grow as indium nanowires which are further oxidized to form single-crystal IONWs with increasing temperature (400–500 °C).¹³ The key point is that the silica monoliths with less external surface areas can make the inorganic species shift completely in the channels and the surfactants serve as both the template and the reducing agent, which successfully resolves the problem of external surface adsorption and makes the template effect more efficient. Contract experiments have also been carried out with calcined SBA-15 as the template, and $\text{In}(\text{NO}_3)_3$ was incorporated by impregnating. After the same thermal treatment and the removal of silica, no mesostructured In_2O_3 was derived, and XRD patterns and TEM showed that large In_2O_3 particles formed at the external surface. Because the doping ratio of In^{3+} is still relatively low, as the SEM image shows, the In_2O_3 mesostructure cannot form with a large domain (about 30% of the channels of the template are filled up), which is also proven by low-angle XRD and the N_2 adsorption/desorption isotherm (see SI). Although the small mesostructure domains are highly ordered, the ordered range is not long enough to yield well-resolved diffraction peaks in low angle range, and only one peak with low intensity is observed. N_2 adsorption/desorption isotherms of the sample show two well-defined steps at P/P_0 of 0.2–0.4 and 0.8–1. The former is caused by the mesopores' adsorption, and a narrow pore-size distribution (average pore diameter of 2.7 nm) confirms the highly ordered uniform pore structure. The latter indicates the stacking holes of the microrods in accordance with the results of SEM and XRD.

In addition, the highly ordered cubic ($Ia3d$ symmetry) single-crystal In_2O_3 mesostructure can also be obtained by the one-step nanocasting method and by using corresponding cubic ($Ia3d$) mesoporous silica monolith as a template.^{11b} The TEM images shown in Figure 2a–c are in three characteristic directions, [100], [111], and [311], and the bicontinuous cubic ($Ia3d$) mesostructure constructed with single-crystal framework is clearly observed. The mesostructured In_2O_3 reported here is a real replica of the cubic $Ia3d$ structure because the silica template possesses 3D mesopores and the nanorods serve as the supporters formed in those pores to

retain the bicontinuous cubic mesostructure.^{14,15} Cubic mesostructured In_2O_3 with possible $I432$ symmetry is also observed in a few domains,^{7,14–15} which may be attributed to the helical pore structure that is not beneficial for the growth of the nanowires and makes the wires form only in one set of the pores. SEM images show a uniform spherulike morphology in the diameter of 200–300 nm for more than 98% of the cubic samples.⁷ XRD and BET characterization results show the long-range structure property similar to that of the hexagonal samples described above (see SI). The BET surface area and the total pore volume are 170 m^2/g and 0.45 cm^3/g , respectively.

The band gap of the mesostructured In_2O_3 framework was measured by UV diffused reflection spectra. As compared with the measured value of the normal bulk In_2O_3 sample (ca. 3.65 eV), both hexagonal and cubic mesostructured In_2O_3 show a wide band gap of ca. 3.93 eV, indicating a weak quantum-confined effect.^{3c}

Furthermore, our results show that this one-step nanocasting synthesis route is a generalized method. We have successfully synthesized highly ordered mesoporous silica monoliths ($p6mm$ and $Ia3d$) with metal oxide (such as Fe_2O_3 , Co_3O_4 , NiO_2 , SnO_2 , ZnO , MnO_2 , CuO) nanocrystals in its channels. The quality of the ordering of the product is much dependent on the melting point for the metal. The lower the point is, the higher the quality is.

In summary, a simple and general one-step nanocasting route has been demonstrated. By using this method, we successfully prepared highly ordered single crystalline In_2O_3 nanowire arrays with hexagonal and cubic mesostructures for the first time. These new materials are believed to be valuable for the potential application in the field of optics and electronics.

Acknowledgment. We thank Y. Chen and H. Jiang for TEM and for N_2 sorption measurements, and we gratefully acknowledge the support of this research by the NSFC (9925309, 20173012, 20233030), State Key Basic Research Program of PRC (2001CB610505), Shanghai Nanotechnology Center (0152nm029, 0144nm067), and Fudan Graduate Innovation Funds.

Supporting Information Available: Detailed characterization results (PDF). This material is available free of charge via the Internet at <http://pubs.acs.org>.

References

- (1) Gordon, R. G. *MRS Bull.* August **2000**, 52.
- (2) Gopchandran, K. G.; Joseph, B.; Abraham, J. T.; Koshy, P.; Vaidyan, V. K. *Vacuum* **1997**, *48*, 547.
- (3) (a) Liang, C.; Meng, G.; Lei, Y.; Philipp, F.; Zhang, L. *Adv. Mater.* **2001**, *13*, 1330. (b) Pan, Z. W.; Dai, Z. R.; Wang, Z. L. *Science* **2001**, *291*, 1947. (c) Murali, A.; Barve, A.; Leppert, V. J.; Risbud S. H.; Kennedy, I. M.; Lee, Howard, W. H. *Nano Lett.* **2001**, *1*, 287.
- (4) Gurlo, A.; Ivanovskaya, M.; Barsan, N.; Schweizer-Berberich, M.; Weimar, U.; Göpel, W.; Diéguez, A. *Sens. Actuators* **1997**, *B44*, 327.
- (5) Schuth, F. *Chem. Mater.* **2001**, *13*, 3184.
- (6) Joo, S. H.; Choi, S. J.; Oh, I.; Kwak, J.; Liu, Z.; Terasaki, O.; Ryoo R. *Nature* **2001**, *412*, 169.
- (7) Shin, H. J.; Ryoo, R.; Liu, Z.; Terasaki, O. *J. Am. Chem. Soc.* **2001**, *123*, 1246.
- (8) Kang, H.; Jun, Y. W.; Park, J. I.; Lee, K. B.; Cheon, J. *Chem. Mater.* **2000**, *12*, 3530.
- (9) Jun, S.; Joo, S. H.; Ryoo, R.; Kruk, M.; Jaroniec, M.; Liu, Z.; Ohsuna, T.; Terasaki, O. *J. Am. Chem. Soc.* **2000**, *122*, 10712.
- (10) Yu, C.; Fan, J.; Tian, B.; Tu, B.; Zhao D. *Adv. Mater.* **2002**, *14*, 1742.
- (11) (a) Yang, H.; Shi, Q.; Tian, B.; Xie, S.; Zhang, F.; Yan, Y.; Tu, B.; Zhao, D. *Chem. Mater.* **2003**, *15*, 536. (b) Yang, H.; Shi, Q.; Liu, X.; Xie, S.; Jiang, D.; Zhang, F.; Yu, C.; Tu, B.; Zhao, D. *Chem. Commun.* **2002**, *23*, 2842.
- (12) Wyckoff, R. W. G. *Crystal Structures*; Interscience: New York, 1968.
- (13) Zheng, M.; Zhang, L.; Zhang, X.; Zhang, J.; Li, G. *Chem. Phys. Lett.* **2001**, *334*, 298.
- (14) Terasaki, O.; Liu, Z.; Ohsuna, T.; Shin, H. J.; Ryoo, R. *Microsc. Microanal.* **2002**, *8*, 35.
- (15) Kameda, M.; Tsubakiyama, T.; Carlsson, A.; Sakamoto, Y.; Ohsuna, T.; Terasaki, O.; Joo, S. H.; Ryoo, R. *J. Phys. Chem. B* **2002**, *106*, 1256.

JA034005I